Journal of Geomatics Vol. 13, No. 1, April 2019

Interannual variation of atmospheric carbon dioxide concentration derived from Orbiting Carbon Observatory-2 (OCO-2) data compared with its local and large-scale variations obtained from NASA Giovanni database

Barun Raychaudhuri* and Tithi Sen Chaudhuri
Department of Physics, Presidency University, Kolkata, India
*Email: barun.physics@presiuniv.ac.in

(Received: Dec 20, 2018; in final form: Jun 01, 2019)

Abstract: The temporal change of global atmospheric carbon dioxide (CO_2) exhibits a positive trend superimposed by an annual cycle, which is ascribed to the combined effect of ecosystem productivity and anthropogenic activities. This work intends to present an analytical treatment of the phenomena in terms of periodicity, local data and their averaging. The time variation of CO_2 concentration derived from NASA-JPL Orbiting Carbon Observatory-2 (OCO-2) database was analyzed with Panoply open source software for two consecutive years 2016 and 2017. The temporal change of the monthly average zonal mean CO_2 flux was obtained from NASA Giovanni earth science database for contrast areas, such as dense forest, desert and crowded city for the period of 2010-16. The results yielded wide differences in the nature of change of both the increasing trend and the seasonal alteration. The Fourier transform indicated the existence of two periodicities superimposed including one sub-annual variation. Possible explanations were given for such general trends in the global change of CO_2. The work was more concentrated on the Indian subcontinent. Prominent difference was found in the positive trend of temporal change at the east coast and the west coast regions over last ten years. The local disparity of CO_2 flux over and around small regions of Northern India exhibited irregular periodic increase and decrease, which when averaged, led to more regular periodicity.

Keywords: Carbon dioxide, OCO-2, NASA Giovanni

1. Introduction

Since the beginning of the industrial age, the concentration of atmospheric carbon dioxide (CO_2) has been increasing at alarming rate. Especially during the last two decades, anthropogenic activities like fossil fuel burning and deforestation have enhanced the CO_2 concentration more rapidly (Etheridge et al., 1996; Leung et al., 2014). Global satellite-borne monitoring systems, such as *Scanning Imaging Absorption Spectrometer for Atmospheric Cartography* (SCIAMACHY) (Bovensmann et al., 1999), *Greenhouse gases Observing Satellite* (GOSAT) (Hamazaki et al., 2004) and *Orbiting Carbon Observatory-2* (OCO-2) (Crisp et al., 2017) and site-specific ground-based systems, such as *Total Carbon Column Observing Network* (TCCON) (Wunch et al., 2011) have been developed for spatial and temporal sampling of atmospheric CO_2 concentration as part of the worldwide mitigation mission for CO_2 emission. Comparative findings of the above sensing systems are reported recently (Wunch et al., 2017; Liang et al., 2017).

The general finding in the temporal change of global atmospheric CO_2 is a positive trend superimposed by an annual cycle, which is ascribed to the combined effect of ecosystem productivity and anthropogenic activities. (Keeling et al.,1976; Basu et al., 2014; Jiang et al., 2016). However, there are wide fluctuations and uncertainties in the rate of CO_2 increase due to various climatic effects, such as natural sink variability (Fu et al., 2017), non-uniform warming (Li et al., 2018), anthropogenic contributions (Xueref-Remy et al., 2018) and wind direction (Roman-Cascon et al., 2019). Accurate monitoring of the above features is necessary for the prediction of future atmospheric CO_2 condition. This work intends to present an analytical treatment of the temporal change in CO_2 in terms of periodicity, local data and their averaging. In particular, the local variations of CO_2 flux over and around small regions of Northern India are studied.

2. Materials and methods

This work utilizes sample data on the spatial and temporal changes of atmospheric CO_2 concentration downloaded from the following two resources. The daily information on CO_2 concentration (ppm) for the years 2016 and 2017 over an area of 22.5º–23.0º N and 86.0º–89.0º E were obtained by using the data produced by the OCO-2 project at the Jet Propulsion Laboratory, California Institute of Technology and obtained from the OCO-2 data archive maintained at the NASA Goddard Earth Science Data and Information Services Center. The monthly averages of CO_2 concentration (ppm) for the period of 2010-16 were procured from NASA Giovanni v4.28 online environments for geophysical parameters.

The Giovanni data were procured for contrast geographic features, such as dense forest, barren desert and crowded urban regions, as mentioned in table 1. More attention was laid on selective places of India, especially those of West Bengal containing Kolkata and around, where ground spectroscopy and airborne imaging were carried out. The OCO-2 data were downloaded with python program and were analyzed with Panoply (v4.9.2) open-source Java application. OCO-2 estimates the column-averaged concentration of atmospheric CO_2 from absorption spectroscopy of reflected solar radiation detected around 0.765 µm (molecular oxygen A band) and two carbon dioxide bands centered around 1.61µm and 2.06 µm. The CO_2 concentration values derived from the 1.61 µm band are used here for analysis. Sorting from the OCO-2 daily database, the concentration values over an area of 22.5º–23.0º N and 86.0º–89.0º E for the Julian days of years 2016 and 2017 were noted for tracking the annual variation. The

spatial variation of CO_2 concentration was derived from AVIRIS-NG image in March 2016 procured for Howrah and Kolkata, regions within and adjacent to the above. The methodology of estimating CO_2 from AVIRIS-NG image is given below in brief.

Table 1: Regions of CO_2 assessment from NASA-Giovanni database

Location	Geographic Feature
27.3°N – 28.83°N 72.7°E – 74.3 °E	Barren Desert
26.2°N – 27.69 °N 70.4°E – 72.5 °E	Barren Desert
26.01°N – 27.5 °N 76.9°E – 78.8 °E	Crowded Urban area
26.26°N – 27.4 °N 80.9°E – 82.7 °E	Crowded Urban area
23.5°N – 24.52 °N 92.17°E – 93.27 °E	Dense Forest
25.4°N – 26.4 °N 92.6°E – 94.5 °E	Dense Forest
27.38°N – 28.52 °N 93.4°E – 95.38 °E	Dense Forest

The reflectance values of different features varied widely but the wavelength dependence for a certain feature did not change much over the CO_2 absorption bands. So the image pixels of differing reflectance for each narrow band were separated by unsupervised classification and the relative differences of the surface reflectance for the pixels of different classes were reduced by multiplying individual pixel values with suitable constants. The pixel values were normalized for path radiance by subtracting the radiance value of pure waterbody pixels having negligible reflectance at these wavelengths. The above algorithm was repeated for each non-absorbing and absorbing AVIRIS-NG band corresponding to CO_2 and O_2 determined from the radiance spectra and the CO_2 concentration was assessed by the usual differential optical absorption spectroscopic (DOAS) technique. Assuming oxygen as one-fifth of the air with a standard molecular density, the CO_2 columnar density was estimated.

3. Results and discussion

Figure 1 displays the variation of atmospheric CO_2 concentration for the period of January, 2016 to December, 2017 retrieved by OCO-2 using the 1.61 µm band for random points, as available, within the region of 22.5º–23.0º N and 86.0º–89.0º E. The data points fitted with Gaussian formula indicate a clear annual cyclic variation in the concentration with the maximum in local summer season. These are the average concentration values over the whole atmospheric column. The results may be compared with the spatial variation of CO_2 concentration shown in figure 2 derived from AVIRIS-NG image (March 2016). The ground level concentration, however, varied over a much wider range, *e.g.* 386–504 ppm (Raychaudhuri and Chaurasia 2017).

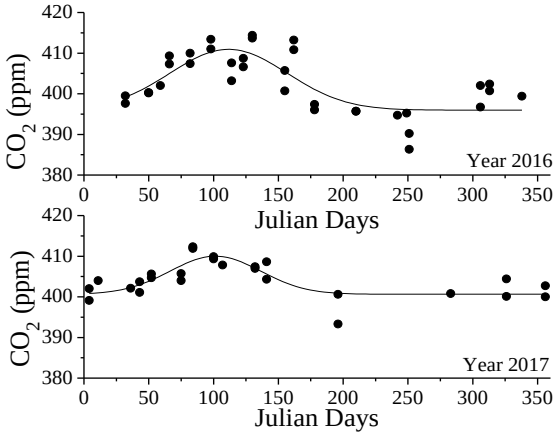

Figure 1: Variation of atmospheric CO_2 concentration within the region of 22.5º–23.0º N and 86.0º–89.0º E for the Julian days of years 2016 and 2017, as retrieved from 1.61 µm band of OCO-2.

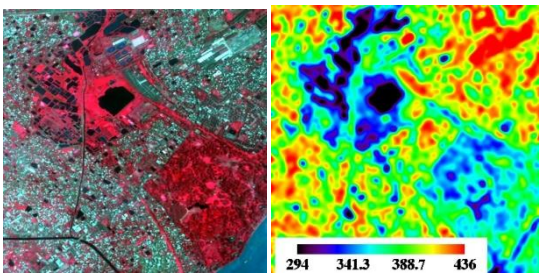

Figure 2: A sample of Spatial variation of CO_2 (ppm) (right panel) for different surface features in RGB image (left panel) derived from AVIRIS-NG image.

The above feature of annual cyclic variation of CO_2 concentration is more illustrated with the long-time variation obtained from Giovanni data. Figure 3 shows the variation of CO_2 concentration during 2010-2016 for individual area of desert (26.27°–27.63°N, 70.34°–72.34°E), urban area (26.01°–27.49°N, 76.95°–78.88°E) and forest (27.38°–28.53°N, 93.45°–95.38°E). Figure 4 presents the variation of CO_2 concentration during 2010-2016 for the east coast (8.68°–8.94°N, 77.76°–78.05°E) and the west coast (8.98°–9.82°N, 76.53°–77.32°E) regions of India.

Discussion on the above results makes it apparent that the CO_2 concentration has a general trend of steady increase with time superimposed by an annual cycle irrespective of geographic features. The annual periodicity becomes more prominent (Figure 3d), when the data are averaged over seven diversified regions of table 1. This explains why the global CO_2 change depicts a well-defined periodicity (Keeling et al., 1976). All the regions related to figure 1 and figure 3 are of tropical climate and exhibit maximum CO_2 flux in summer season. Also there is difference in the temporal steady increase. Figure 4 deals with the CO_2 concentration over the two coastal regions of the same Indian peninsula. Both the regions undergo steady CO_2 increase superimposed by its annual seasonal fluctuation. However, because of difference in geographic and climatic conditions, the data fitted with straight line result in prominent difference in the slopes indicating different rates of CO_2 increase for these two regions.

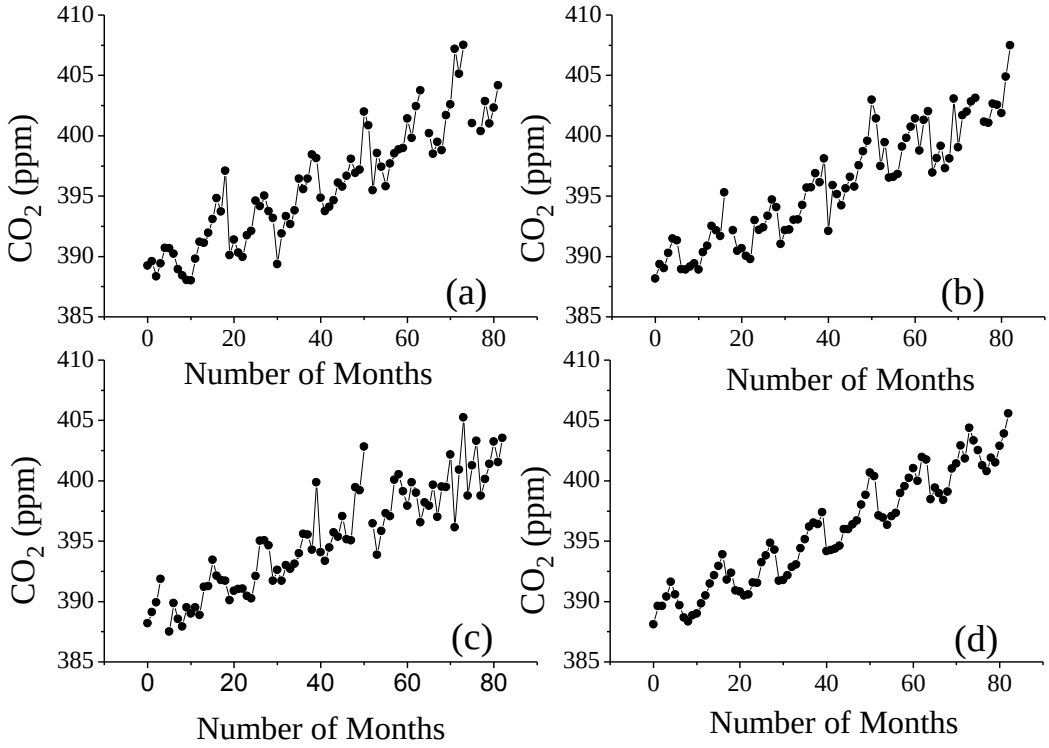

Figure 3: Annual variation of atmospheric CO_2 concentration during 2010-2016 for individual area of (a) desert, (b) urban area, (c) forest and (d) average of seven such regions given in table 1.

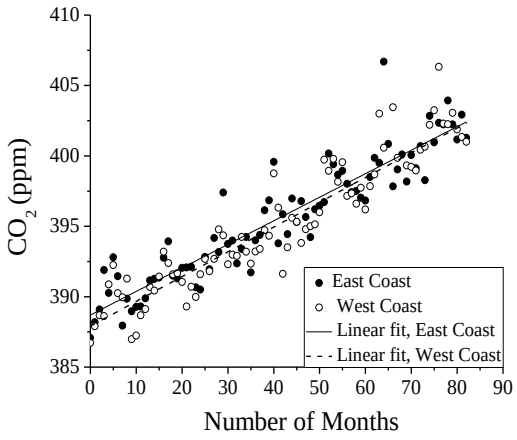

Figure 4: CO_2 concentration during 2010-2016 for the east and west coast regions of India

For the sake of subtler investigation, the linear increment part of the average CO_2 in figure 3d was eliminated and Fourier transform was carried out for the seasonal alteration, as shown in figure 5. It is noted that in addition to the prominent yearly periodicity caused by the regular annual climatic change, there exists a secondary semi-annual peak and also other weaker peaks. Thus the resultant temporal change in CO_2 flux is the combined effect of several factors, such as local climatic change, CO_2 uptake by vegetation and man- made changes.

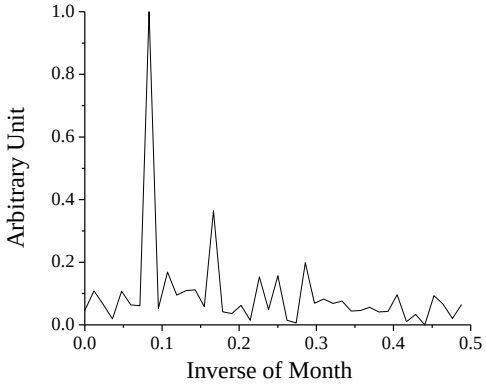

Figure 5: Fourier transform of the CO_2 seasonal periodic component obtained from figure 3d

4. Conclusions

The variation of atmospheric CO_2 concentration (ppm) during 2016-17 at around Kolkata was tracked using OCO-2 data archive and the extent of concentration was compared with that obtained from AVIRIS-NG image. An annual cyclic change in the CO_2 concentration was noted. In order to find the trend of such change during the last one decade, the monthly average values from Giovanni data archive were extracted for several places of contrast geographic features in India. A steady increase in CO_2 concentration was noted for all the places but the periodicity was not well defined. Local variation in the rate of increase was also noted. However, it is found that on

averaging the local values over several such places, the annual periodicity became more prominent as obtained in the global trend. Several periodicities were found to be present in the annual change of CO_2 flux from Fourier transform of the temporal change.

Acknowledgements

The authors thankfully acknowledge the financial support of Space Applications Centre, Indian Space Research Organization (vide AVIRIS-NG AO Project Ref. EPSA/4.20/2017 dt. 19.12.2017) and the infrastructural facilities extended by Presidency University. The authors thankfully acknowledge the use of OCO-2 and Giovanni data mentioned in the text.

References

Basu, S., M. Krol, A. Butz, C. Clerbaux, Y. Sawa, T. Machida, H.Matsueda, C. Frankenberg, O. P. Hasekamp and I. Aben (2014). The seasonal variation of the CO_2 flux over Tropical Asia estimated from GOSAT, CONTRAIL, and IASI, Geophysical Research Letters 41, 1809-1815.

Bovensmann, H., J.P. Burrows, M. Buchwitz, J. Frerick, S. Noel and V.V. Rozanov (1999). SCIAMACHY: Mission objectives and measurement modes, Journal of the Atmospheric Sciences 56, 127-150.

Crisp, D et al., (2017). The on-orbit performance of the Orbiting Carbon Observatory-2 (OCO-2) instrument and its radiometrically calibrated products, Atmospheric Measurement Techniques 10, 59-81.

Etheridge, D.M., L.P. Steele, R.L. Langenfelds, R.J. Francey, J.-M. Barnola and V.I. Morgan (1996). Natural and anthropogenic changes in atmospheric CO_2 over the last 1000 years from air in Antarctic ice and firn., Journal of Geophysical Research 101(D2), 4115-4128.

Fu, Z., J. Dong, Y. Zhou, P. C. Stoy and S. Niu (2017). Long term trend and interannual variability of land carbon uptake – the attribution and processes, Environmental Research Letters 12, p. 014018.

Hamazaki, T., Y. Kaneko and A. Kuze (2004). Carbon dioxide monitoring from the GOSAT satellite. Proceedings of XXth ISPRS Conference 3-5, Istanbul, Turkey, July 12-13, 2004.

Jiang, X., D. Crisp, E.T. Olsen, S.S. Kulawik, C.E. Miller, T. S. Pagano, M. Liang and Y. L. Yung (2016). CO_2 annual and semiannual cycles from multiple satellite retrievals and models, Earth and Space Science, 3(2), 78-87.

Keeling, C., R.B. Bacastow, A.E. Bainbridge, C.A. Ekdahl, Jr, P.R. Guenther and L.S. Waterman (1976). Atmospheric carbon dioxide variations at Mauna Loa Observatory, Hawaii, Tellus, 28(6), 538-551.

Leung, D.Y.C., G. Caramanna and M.M. Maroto-Valer (2014). An overview of current status of carbon dioxide capture and storage technologies, Renewable and Sustainable Energy Reviews, 39, 426-443.

Li, Z et al., (2018). Non-uniform seasonal warming regulates vegetation greening and atmospheric CO_2 amplification over northern lands, Environmental Research Letters, 13, 124008.

Liang, A., W. Gong, G. Han and C. Xiang (2017). Comparison of Satellite-Observed XCO2 from GOSAT, OCO-2, and Ground-Based TCCON, Remote Sensing, 9, 1033-1059.

Raychaudhuri, B. and S. Chaurasia (2017). Ground-based hyperspectral measurement at visible-infrared wavelengths for validation of the atmospheric carbon dioxide absorption wavebands in the context of AVIRIS-NG flight over Kolkata-Howrah, Journal of Geomatics 11(2), 167-173.

Roman-Cascon, C., C. Yague, J. A. Arrillaga, M. Lothon, E. R. Pardyjak, F. Lohou, R. M. Inclan, M. Sastre, G. Maqueda, S. Derrien, Y. Meyerfeld, C. Hang, P. Campargue-Rodriguez and I. Turki (2019). Comparing mountain breezes and their impacts on CO_2 mixing ratios at three contrasting areas, Atmospheric Research, 221, 111-126.

Wunch, D., G. C. Toon, J.-F. L. Blavier, R. A. Washenfelder, J. Notholt, B. J. Connor, D. W. T. Griffith, V. Sherlock and P. O. Wennberg (2011). The Total Carbon Column Observing Network, Philosophical Transactions of the Royal Society A: Mathematical, Physical and Engineering Sciences, 369(1943), 2087-2112.

Wunch, D et al., (2017). Comparisons of the Orbiting Carbon Observatory-2 (OCO-2) X_{CO2} Measurements with TCCON, Atmospheric Measurement Techniques 10, 2209-2238.

Xueref-Remy, I., E. Dieudonné, C. Vuillemin, M. Lopez, C. Lac, M. Schmidt, M. Delmotte, F. Chevallier, F. Ravetta, O. Perrussel and P. Ciais (2018). Diurnal, synoptic and seasonal variability of atmospheric CO_2 in the Paris megacity area, Atmospheric Chemistry and Physics, 18, 3335-3362.